

RESEARCH PAPER

Coating doxorubicin-loaded nanocapsules with alginate enhances therapeutic efficacy against *Leishmania* in hamsters by inducing Th1-type immune responses

S Kansal^{1*}, R Tandon^{2*}, A Verma¹, P Misra², A K Choudhary², R Verma¹, P R P Verma³, A Dube² and P R Mishra¹

¹Pharmaceutics Division, CSIR-Central Drug Research Institute, BS-10/1 sector-10 Jankipuram Extension, Lucknow, India, ²Parasitology Division, CSIR-Central Drug Research Institute, BS-10/1 sector-10 Jankipuram Extension, Lucknow, India, and ³Department of Pharmaceutical Science, Birla Institute of Technology, Mesra, Ranchi, India

Correspondence

Prabhat Ranjan Mishra,
PCS-002/011-Preclinical south,
CSIR-Central Drug Research
Institute, BS-10/1 sector-10
Jankipuram Extension, Lucknow
226001, India. E-mail:
mishrapr@hotmail.com;
prabhat_mishra@cdri.res.in

*Both authors contributed
equally.

Received

14 November 2013

Revised

9 April 2014

Accepted

23 April 2014

BACKGROUND AND PURPOSE

The aim of the present study was to evaluate the immunomodulatory and chemotherapeutic potential of alginate-(SA) coated nanocapsule (NCs) loaded with doxorubicin (SA-NCs-DOX) against visceral leishmaniasis in comparison with nano-emulsions containing doxorubicin (NE-DOX).

EXPERIMENTAL APPROACH

NE-DOX was prepared using low-energy emulsification methods. Stepwise addition of protamine sulphate and SA in a layer-by-layer manner was used to form SA-NCs-DOX. SA-NCs-DOX, NE-DOX and Free DOX were compared for their cytotoxicity against *Leishmania donovani*-infected macrophages *in vitro* and generation of T-cell responses in infected hamsters *in vivo*.

KEY RESULTS

Size and ζ potential of the NE-DOX and SA-NCs-DOX formulations were 310 ± 2.1 nm and (-32.6 ± 2.1) mV, 342 ± 4.1 nm and (-29.3 ± 1.2) mV respectively. SA-NCs-DOX was better (1.5 times) taken up by J774A.1 macrophages compared with NE-DOX. SA-NCs-DOX showed greater efficacy than NE-DOX against intramacrophagic amastigotes. SA-NCs-DOX treatment exhibited enhanced apoptotic efficiency than NE-DOX and free DOX as evident by cell cycle analysis, decrease in mitochondrial membrane potential, ROS and NO production. T-cell responses, when assessed through lymphoproliferative responses, NO production along with enhanced levels of iNOS, TNF- α , IFN- γ and IL-12 were found to be up-regulated after SA-NCs-DOX, compared with responses to NE-DOX *in vivo*. Parasitic burden was decreased in *Leishmania*-infected hamsters treated with SA-NCs-DOX, compared with NE-DOX.

CONCLUSIONS AND IMPLICATIONS

Our results provide insights into the development of an alternative approach to improved management of leishmaniasis through a combination of chemotherapy with stimulation of the innate immune system.

Abbreviations

CMI, cell-mediated immunity; DLS, dynamic light scattering; DOX, doxorubicin; EE, entrapment efficiency; HRTEM, high-resolution transmission electron microscopy; LBL, layer-by-layer; LTT, lymphoproliferative responses; MTT, (3-[4, 5-dimethylthiazol-2-yl]-2, 5-diphenyltetrazolium bromide); NCs, nanocapsules; NE-DOX, nano-emulsion containing doxorubicin; PRM, protamine sulfate; PSS, poly-sodium 4 -styrenesulfonate; SA, sodium alginate; SA-NCs-DOX, doxorubicin-loaded sodium alginate-coated nanocapsules; SBO, soyabean oil; SLD, soluble *L. donovani* antigen; VL, visceral leishmaniasis

Introduction

Current treatments for visceral leishmaniasis (VL) are unsatisfactory because of their toxicity, resistance and high cost (Sundar and Rai, 2002; Ghosh *et al.*, 2011). In VL, the parasites infect and reside in macrophages, thereby evading host defence mechanisms and this sheltered location prevents the access of chemotherapeutic agents to the parasites. Most of the anti-leishmanial drugs presently in use fail to penetrate macrophages containing parasites and this has driven pharmaceutical research to develop better drug delivery systems for more effective therapeutic response. The standard anti-leishmanial chemotherapy consists of antimony-based compounds but response to these drugs is failing because of the emergence of resistance and the accompanying frequent relapses (Tiuman *et al.*, 2011). Pentamidine and amphotericin B are the second-line treatment of leishmaniasis after antimony failure, but their use is also limited because of their adverse effects (Halder *et al.*, 2011; Oliveira *et al.*, 2011). The combination of drug-resistant *Leishmania* strains and the consequent rising financial burden has produced an urgent need for new therapeutic agents. One approach to counteract the emerging trend of multi-drug resistant VL is to exploit the host's own non-specific, innate responses against leishmaniasis as a therapeutic effect.

There is an urgent need for alternative safe delivery systems for existing molecules, which would increase the efficacy and reduce the dose-related toxicity of these agents to the phagosomes of reticuloendothelial macrophages where the *Leishmania* resides. Moreover, the liposomal formulations recommended by the US Food and Drug Administration are too costly for developing countries. All these factors emphasize the need to develop a robust, affordable and storage-stable drug delivery system incorporating a large payload of the anti-leishmanial agent. The present project was undertaken as a combination of 'proof-of-principle' and a preclinical product development exercise, culminating in the preparation of a prototype formulation that preferentially stimulates innate immune responses of *Leishmania*-infected macrophages, in addition to targeting them with a bolus of anti-leishmanial agent.

The well studied anthracycline doxorubicin (DOX), used for the chemotherapy of various human cancers, was found to exert anti-leishmanial activity, but its associated cardiac toxicity limited its clinical use (Sett *et al.*, 1992; Gupta *et al.*, 2009). DOX has been shown to induce apoptosis in the *Leishmania* parasite (Singh and Dey, 2007; Luanpitpong *et al.*, 2012) and, recently, was found to activate immune functions of macrophages and NK cells (Hussner *et al.*, 2012). Immuno-intervention with antimonials, amphotericin B and DOX is known to improve VL (Murray *et al.*, 2003a; Mukherjee *et al.*,

2004), but toxicity remains a major concern. The biopolymers, sodium alginate (SA) and chitosan are potent activators of macrophages, inducing the release of a range of cytokines and cytotoxic agents (Porporatto *et al.*, 2003; Yang and Jones, 2009; Singodia *et al.*, 2011). Higuchi *et al.* (1990) demonstrated that TNF- α and L-arginine-derived NO act synergistically to produce cytotoxicity in macrophages. Thus the development of a formulation using biocompatible polymers, which enhances immunological responses might provide a new approach to improved treatment of leishmaniasis.

We found that DOX-loaded SA-coated nanocapsules (SA-NCs-DOX) improved the anti-leishmanial efficacy of the drug by increasing the uptake of DOX by *Leishmania donovani*-infected macrophages and by increasing the activation of macrophages leading to release of cytokines and reactive oxygen species (ROS).

Methods

Preparation of nano-emulsions (NE)

The low-energy emulsification method was utilized to prepare NE as reported previously (Kansal *et al.*, 2012). In brief, NE was obtained from a mixture of SBO (20 wt %) containing free DOX base and Span 80/Tween 80 (weight ratio of approximately 0.43/0.57) by slowly adding aqueous phase containing PSS (0.025 wt %) at a flow rate of 1 mL·min⁻¹ with gentle agitation using a magnetic stirrer at a temperature of 60°C. Free DOX base was obtained as follows; DOX extraction in chloroform was carried out in the presence of triethylamine (3 mol equivalents to DOX-HCl) (Kataoka *et al.*, 2000). The aqueous phase was shaken with chloroform for 24 h at 25°C. Then, chloroform was evaporated under vacuum to a final volume of 1 mL which was then mixed with SBO and kept in the dark.

Preparation of SA-coated NCs

The NE mentioned earlier serves as core template for the preparation of polyelectrolyte-coated NCs. Thus, in the pre-formed NE, 10 mL of an aqueous polyelectrolyte solution of protamine sulfate (PRM; 0.125% w/v) was injected and stirred for 45 min. For the preparation of SA-NCs, the procedure was repeated to coat oppositely charged SA (0.150% w/v). Then, the dispersion was centrifuged for 20 min at 40 000× *g* to separate the NCs from non-encapsulated polyelectrolyte aggregates.

Characterization of NE and SA-NCs

Size, ζ potential and surface characterization. Particle size and ζ potential of formulations were determined by a Nano-ZS ζ sizer (Malvern Instruments, Malvern, UK) at 25°C. The

analysis was carried out on both NE and SA-NCs, within 2 h after their preparation. The formulation was diluted appropriately with distilled water prior to analysis, and each measurement was carried out in triplicate. The polydispersity index was obtained by the instrument's built-in software. The surface morphology of optimized NCs was studied through high-resolution transmission electron microscopy (HRTEM, G², F20, Tecnai, Eindhoven, the Netherlands). For HRTEM, the sample was prepared as a thin aqueous film supported on 300-mesh copper grid. Negative staining was done using 2% w/v phosphotungstic acid. Direct imaging of samples was done at a 200 kV acceleration voltage on HRTEM.

Percentage of entrapment efficiency (% EE) measurement. The amount of DOX entrapped was determined as follows: 1.5 mL of 0.1M HCl was added to 0.5 mL freshly prepared DOX formulations. Then the mixture was centrifuged at 40 000× g and 4°C for 30 min. Then 1 mL of the aqueous phase was carefully removed with a 2 mL hypodermic syringe. The solution was filtered with a Millipore filter (0.22 µm in pore size) and drug content was analysed by reverse-phase HPLC method (Hartmann *et al.*, 2005).

$$\% \text{Entrapment} = \frac{(\text{total amount of drug} - \text{free drug})}{\text{total amount of drug}} \times 100$$

In vitro evaluation against intramacrophage amastigotes of *L. donovani*. The J774A.1 macrophages (National Centre for Cell Science (NCCS), Pune, India) were resuspended at 2.5×10^5 cells·mL⁻¹ in serum-free RPMI-1640. Two hundred microlitre cell suspensions per well were plated on an eight-chamber Lab-Tek tissue culture slides (Nunc, Thermo Scientific, Naperville, IL, USA) and allowed to adhere for 2 h in a CO₂ incubator at 37°C. Wells were washed twice with serum-free medium, and the adherent macrophages were infected with stationary stage parasites of *L. donovani* maintaining a *Leishmania*/macrophage ratio of 10:1 in complete medium and incubated overnight. After 24 h, free promastigotes were washed with serum-free medium and infected macrophages were incubated with medium containing Free DOX, NE-bearing DOX (NE-DOX) and SA-NCs-DOX at various concentrations (0.1, 0.2, 0.3, 0.5, 1.0 and 2.0 µg·mL⁻¹) for 48 h at 37°C. Untreated infected macrophages served as control. The slides were fixed with methanol and stained with Giemsa. The IC₅₀ was obtained by plotting a graph of the percentage of inhibition at different concentrations of all the observations using Origin 6.1 version software (OriginLab, Northampton, MA, USA) and expressed in µg·mL⁻¹ (Pal *et al.*, 1991).

Macrophage uptake studies

The adherent mouse macrophage cell line J774A.1 was used for this study. Aliquots (100 µL) containing J774A.1 cells (1×10^5) were suspended in 0.9 mL of RPMI-1640 medium with 10% FBS (Duverger *et al.*, 2006). These were transferred into 24-well plates (Corning, Costar, NY, USA) containing fresh medium and suspended in a 37°C humidified incubator with 5% CO₂ atmosphere. After 24 h, the culture medium was replaced with fresh culture medium containing NE-DOX and SA-NCs-DOX formulations. For separation of the internalized and surface-bound NCs, the cells were washed three times with acetate buffer (pH 4.0). The cell-associated fluorescence

was measured by FACS (BD Biosciences, FACS Aria, Germany) at an excitation wavelength of 480 nm and an emission wavelength of 550 nm (Albright *et al.*, 2005).

Cytotoxicity studies

The *in vitro* cytotoxicity of control (not containing DOX) formulations was measured by the MTT proliferation assay (Seymour *et al.*, 1994). The experiments were carried out on cells in the exponential growth phase. J774A.1 and RAW macrophages (NCCS) were seeded into 24-well plates at 5×10^4 cells per well and were allowed to adhere overnight. The growth medium was replaced with a fresh medium and incubated for 24 h with different formulations (NE and SA-NCs). Cells washed twice with PBS were then incubated in a growth medium containing 1 mg·mL⁻¹ MTT for 4 h at 37°C, and then 500 µL DMSO was added to each well to ensure solubilization of the formazan crystals. The optical density was measured using a multi-well scanning spectrophotometer (MRX Microplate Reader, Dynatech Laboratories Inc., Chantilly, VA, USA) at a wavelength of 570 nm.

Flow cytometric analysis of cell cycle

DNA fragmentation during apoptosis by Free DOX and its formulations was measured by cell cycle analysis through flow cytometry (Soto *et al.*, 2004; Riccardi and Nicoletti, 2006). Briefly, 10^6 promastigotes were seeded in 24-well plates (Corning) and treated with 0.5 µg·mL⁻¹ of each of the free drug, NE-DOX and SA-NCs-DOX. After 24 h cells were harvested by centrifugation at 35 000× g, washed twice with PBS, re-suspended in 1 mL of fixative solution (30% PBS/70% methanol) and incubated at 4°C for 1 h. Afterwards, parasites were collected by centrifugation, resuspended in PBS containing 20 µg·mL⁻¹ of RNaseA (Fermentas, Henover, MD, USA) and incubated for 20 min at 37°C. After incubation, the cells were harvested, resuspended in 1 mL of citrate buffer (45 mM MgCl₂; 30 mM sodium citrate; 20 mM MOPS; 0.1% Triton X-100; at pH 7.0), and stained by the addition of 50 µg of propidium iodide (Sigma) followed by incubation at 37°C for 20 min. Afterwards, stained cells were washed twice with PBS containing 5% foetal calf serum. The samples were stored at 4°C in the dark until analysis. Fluorescence was determined by flow cytometry on a flow cytometer (Beckman Coulter FC 500, Brea, CA, USA).

Mitochondrial membrane potential ($\Delta\psi$ m) determination

Briefly, promastigotes were collected after treatment with drug and the formulations for various time periods and incubated for 7 min with 10 mM JC-1 (Sigma-Aldrich) at 37°C, washed and resuspended in medium. The ratio of fluorescence at 590–530 nm was considered to be the relative $\Delta\psi$ m value (Dey and Moraes, 2000).

Estimation of levels of ROS

To evaluate the generation of ROS in promastigotes and infected macrophages following treatment with Free DOX, NE-DOX and SA-NCs-DOX the cell-permeant probe 2',7'-dichlorodihydrofluorescein diacetate (H₂DCFDA) was used (Duranteau *et al.*, 1998). Cells treated with DOX and NCs-DOX for different time periods were resuspended in 500 µL

RPMI 1640 and labelled with 10 μM H_2DCFDA for 15 min in the dark. Cells were analysed for intracellular ROS by using flow cytometer.

Measurement of NO production in infected macrophages

The Griess reagent was used to measure nitrite (NO_2^-) in the culture supernatants of infected macrophages, after treatment with all formulations. Briefly, J774A.1 macrophages infected with *L. donovani* parasites were treated with Free DOX, NE-DOX and SA-NCs-DOX. The supernatants (100 μL) collected from macrophage cultures at 12 and 24 h after incubation was mixed with an equal volume of Griess reagent (Sigma) and left for 10 min at room temperature (RT). The absorbance of the reaction was measured at 540 nm (Tandon *et al.*, 2012).

In vivo studies

Animals. All animal care and experimental use conformed to Committee for the Purpose of Control and Supervision on Experiments on Animals guidelines for laboratory animal facilities and were approved by the Committee on the Ethics of Animal Experiments of the Central Drug Research Institute. All studies involving animals are reported in accordance with the ARRIVE guidelines for reporting experiments involving animals (Kilkenny *et al.*, 2010; McGrath *et al.*, 2010). A total of 5 animals were used in the experiments described here.

Laboratory-bred male golden hamsters (*Mesocricetus auratus*, 45–50 g) from the Institute's animal house facility were used as the experimental host. They were housed in climatically controlled rooms ($24 \pm 2^\circ\text{C}$ and 45–60% humidity) and fed with standard rodent food pellets (Lipton India, Ltd., Mumbai, India) and water *ad libitum* (Tandon *et al.*, 2012). The experimental animals were monitored daily till the end point of the study and were autopsied at the end-point by deep anaesthesia with over dosages of sodium thio-pentone (50 $\text{mg}\cdot\text{kg}^{-1}$) in order to reduce the suffering level in experimental animals.

Anti-leishmanial activity testing. The isolation of parasites and infection to naïve hamsters were carried out as described earlier (Gupta *et al.*, 2011). Infected animals ($n = 5$) harbouring 38–40 amastigotes/100 macrophage nuclei were then distributed with six animals in each group for drug treatment in the following manner: (i) infected controls (no therapy was given); (ii) Free DOX; (iii) NE-DOX; (iv) SA-NCs-DOX; (v) control (no DOX) NE; and (vi) control SA-NCs.

Infected hamsters were treated i.p. with 250 $\mu\text{g}\cdot\text{kg}^{-1}$ per day of DOX and all its formulations for 4 consecutive days. After 30 days of treatment, splenic biopsies were performed and parasite burden was determined by counting the number of amastigotes (Guru *et al.*, 1989).

Measurement of lymphoproliferative responses (LTT) and NO production

The cellular responses of lymph node cells of experimental animals to the mitogens, concanavalin A (Con A) and LPS, were assessed by the lymphoproliferative responses (LTT) and NO production, respectively, and soluble *L. donovani* antigen

(SLD), as described elsewhere (Samant *et al.*, 2009) with some modifications in which we used XTT (Roche Diagnostics, Mannheim, Germany) instead of [^3H] thymidine. Eighteen hours prior to termination of the experiment, XTT (50 μL) was added to 100 μL of the supernatant of each well and absorbance was measured at 480 nm with 650 nm as the reference wavelength. To estimate NO production, nitrite accumulation in culture supernatants of hamster peritoneal macrophages was determined by the Griess reagent, as described elsewhere (Gupta *et al.*, 2011).

Measurement of anti-leishmanial antibody responses

Anti-leishmanial antibody levels of IgG and its isotypes IgG1 and IgG2 were assessed using sera from all the experimental groups collected on day 30 of treatment. as described by Samant *et al.* (2009), with slight modifications. Briefly, 96-well ELISA plates (Nunc) were coated with SLD ($0.2 \mu\text{g}\cdot 100 \text{ mL}^{-1}$ per well) overnight at 4°C and blocked with 1.5% BSA at room temperature for 1 h. Sera were used at a dilution of 1/100 and kept for 2 h at room temperature. After washing, biotin-conjugated mouse anti-Armenian and Syrian hamster IgG, IgG1 and biotinylated anti-Syrian hamster IgG2 (BD Pharmingen, San Diego, CA, USA) were added for 1 h at room temperature at 1/1000 dilution and were further incubated with peroxidase-conjugated streptavidin at 1/1000 (BD Pharmingen) for 1 h. Finally, the substrate O-phenylenediamine dihydrochloride (Sigma-Aldrich) was added and the plate was read at 492 nm.

Estimation of expression of mRNA cytokines by real-time PCR in treated hamsters

Real-time PCR was performed to evaluate the expression of mRNAs for several cytokines and inducible NOS in splenic cells. Splenic tissues were removed from each of the three individual animals randomly chosen from different groups. Total RNA was isolated using Tri reagent (Sigma-Aldrich) and 1 μg of total RNA was used for the synthesis of cDNA using a first-strand cDNA synthesis kit (Fermentas). For real-time PCR, primer sequences and protocol were used as described earlier (Samant *et al.*, 2009). cDNAs from infected hamsters were used as 'comparator samples' for quantification of those corresponding to test samples. All quantifications were normalized to the housekeeping gene *HGPRT*. A no-template control cDNA was included to eliminate contaminations or non-specific reactions. The cycle threshold (C_T) value was defined as the number of PCR cycles required for the fluorescence signal to exceed the detection threshold value (background noise). Differences in gene expression were calculated by the comparative C_T method (Samant *et al.*, 2009). This method compares test samples to a comparator sample and uses results obtained with a uniformly expressed control gene (*HGPRT*) to compensate for deviations in the amounts of RNA present in the two samples being compared with generate a ΔC_T value. Results are expressed as the degrees of difference between ΔC_T values of test and comparator samples.

Data analysis

All results are given as means \pm SD ($n = 3$). Differences between formulations were compared using one-way ANOVA followed by the Turkey–Kramer multiple comparison test,

using GraphPad InStat software (Graph Pad Software, Inc., La Jolla, CA, USA). $P < 0.05$ denotes significance in all cases.

Materials

DOX was received as a gift from Dabur Research Foundation, Ghaziabad, India. Protamine sulfate (PRM), poly-sodium 4 -styrenesulfonate (PSS; MW 70 000) and 3-[4, 5-dimethylthiazol-2-yl]-2, 5-diphenyltetrazolium bromide (MTT) were purchased from Sigma-Aldrich (St. Louis, MO, USA). Tween 80 and Span 80 were procured from HiMedia Laboratories Pvt., Ltd., Mumbai, India. Soyabean oil (SBO) was purchased from Sunshine Oleochem, Ltd., Gandhidham, India. All other chemicals and solvents were of analytical grade.

Results

Preparation and characterization

The low-energy emulsification method was used to prepare NE, which served as a template for depositing additional polyelectrolytes on the surface to form NCs. This procedure represents an innovative and preferable manner of production of polyelectrolyte NCs. In a first step, the NE (oil/water) was obtained from a mixture of SBO (20 wt %) and ratio of surfactants (Span 80/Tween 80 approximately 0.43/0.57) by slowly adding aqueous phase at a rate of $1 \text{ mL} \cdot \text{min}^{-1}$ with gentle agitation using a magnetic stirrer on heating. In the second step, alternating addition of PRM and SA layers leads to the formation of SA-NCs (outermost layer of SA) with a NE core. The rigidity of the shell and the ζ potential were also found to depend on the concentration of PRM and SA.

The EE in NE formulations was over 80% (Table 1) and making the NCs, coated with polyelectrolyte with SA as the outer layer, did not significantly affect the % EE. The uncoated NE was negatively charged because of the PSS (ζ -potentials shown in Table 1) and, on deposition of the initial PRM layer, the charge was reversed to (+) $39.2 \pm 3.9 \text{ mV}$, while after subsequent layering with SA, the ζ potential fell to negative values, as expected, and not very different from that of the NE (Table 1). Depending on the type of polyelectrolyte added, the ζ potential altered at every layering, confirming layer-by-layer (LBL) assembly of the coating over the NE core. The particle size and size distributions of different formulations were measured by dynamic light scattering (DLS). HRTEM showed the structure of NCs (Figure 1) as having a hollow core with a smooth texture on the surface.

Table 1

Characterization of SA-NCs-DOX and NE-DOX formulations

Formulation	Charge (mV)	Size (nm)	% Entrapment efficiency
NE-DOX	(-32.6 ± 2.1)	310 ± 2.1	84 ± 4.2
SA-NCs-DOX	(-29.3 ± 1.2)	342 ± 4.1	82 ± 6.3

In vitro evaluation against intramacrophage amastigotes of *L. donovani*

Inhibition of amastigote multiplication within macrophages by Free DOX, NE-DOX and SA-NCs-DOX was measured (Figure 2). All samples were stained, and the number of infected macrophages was determined microscopically. Both the nano-formulations, NE-DOX and SA-NCs-DOX, showed improved efficacy, compared with Free DOX. Also, SA-NCs-DOX was more effective than NE-DOX.

In vitro uptake studies

Figure 3 shows the uptake of the DOX formulations by J774A.1 macrophage cells, assessed by flow cytometry. This study compared the uptake of Free DOX, NE-DOX and SA-NCs-DOX. Figure 3 shows almost 2.5-fold greater uptake of NE-DOX than of Free DOX, while the SA-NCs-DOX formulation was taken up almost 1.5-fold more than NE-DOX.

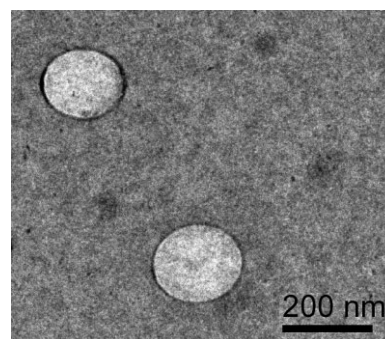


Figure 1

High-resolution transmission electron microphotograph of doxorubicin-loaded NCs.

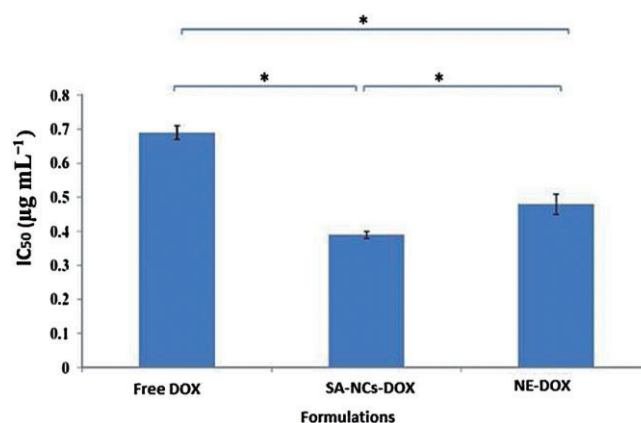


Figure 2

In vitro activity of DOX formulations on *L. donovani* intramacrophagic amastigotes. Results are expressed as inhibition of parasite growth (IC₅₀) observed after 48 h of incubation with Free DOX, NE-DOX or SA-NCs-DOX. Data shown are means \pm SD of three sets of experiments ($n = 3$). * $P < 0.01$, significantly different as indicated.

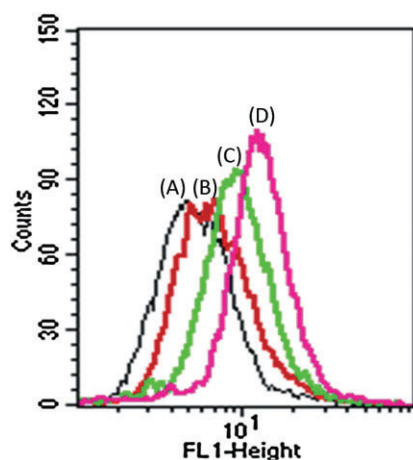


Figure 3

Flow cytometric diagram for uptake studies in macrophagic J774A.1 cells. X-axis represents fluorescence inside the cells. Figure shows the fluorescence in (A) control cells, in cell treated with (B) Free DOX, (C) NE-DOX or (D) SA-NCs-DOX.

SA-NCs-DOX exhibited greater apoptotic efficiency than Free DOX and NE-DOX

In these experiments, we compared the apoptotic efficacy of SA-NCs-DOX and NE-DOX with the free drug, against *L. donovani* promastigotes. Digestion of DNA into oligonucleosomal fragments is a marker of classical apoptosis and cells undergoing this chromatin alteration become pseudohypodiploid cells. Flow cytometry analysis after cell permeabilization and labelling with PI was used to quantify the percentage of pseudohypodiploid cells. The amount of bound dye correlates with the DNA content in a given cell, and DNA fragmentation in apoptotic cells translates into a fluorescence intensity lower than that of G1 cells (sub-G1 peak). After 24 h of incubation of promastigotes with SA-NCs-DOX, a third of the cells were found in the sub-G1 peak region whereas only 15 and 23% of the total cells treated with Free DOX and NE-DOX, respectively, were found in the sub-G1 peak region (Figure 4Ai and Aii). These results showed that SA-NCs-DOX had induced more DNA degradation in promastigotes, compared with NE-DOX and Free DOX.

Mitochondrial membrane potential ($\Delta\psi_m$) determination

Earlier studies have shown that the mitochondrion is a possible target of ROS-induced apoptosis in *Leishmania*, corresponding to the fall in $\Delta\psi_m$ (Sudhandiran and Shaha, 2003). Simultaneous measurement of the J-aggregate (indicative of intact mitochondria) and J-monomer (indicative of de-energized mitochondria) showed a sharp fall during 6–24 h after treatment with all compounds (Figure 4B). However, the greatest fall in $\Delta\psi_m$ was observed with SA-NCs-DOX treatment, compared with Free DOX or NCs-DOX at all time points.

Estimation of ROS and NO levels

H₂DCFDA, a non-polar compound, is converted on oxidation to the highly fluorescent 2',7'-dichlorofluorescein and this

property has been utilized to monitor ROS generation. SA-NCs-DOX treatment of promastigotes led to a maximum increase in ROS at all time points up to 24 h, followed by NE-DOX and Free DOX (Figure 4Di and Dii). Similar results were obtained while measuring NO levels in which cells exposed to SA-NCs-DOX showed the highest NO generation, compared with Free DOX and NE-DOX treatments, at 12 h and 24 h (Figure 4C).

In vivo anti-leishmanial activity testing

Anti-leishmanial activity in vivo was assayed as inhibition of the parasite burden in spleen samples taken from infected animals after treatment. This burden was most effectively inhibited by SA-NCs-DOX, compared with NE-DOX or Free DOX (Figure 5) in hamsters infected with *L. donovani*. Control SA-NCs also induced significant inhibition, less than any formulation containing DOX but still greater than that induced by control NE (Figure 5).

Leishmania-specific LTT, NO and antibody responses in treated hamsters

We observed that *in vitro* stimulation of the lymphocytes isolated from lymph nodes with ConA, as well as SLD, showed the maximum LTT in the cells of animals treated with SA-NCs-DOX (Figure 6A), which was significantly higher than that to Free DOX or NE-DOX-treated animals. Similarly, the generation of NO observed in the SA-NCs-DOX group was the highest of all the treated groups (Figure 6B).

In VL, levels of antibody to the parasite correlate with the intensity of infection harboured by the host. On day 30 of treatment, the anti-*Leishmania* IgG was elevated in the infected group and was decreased significantly in the group with SA-NCs-DOX treatment, followed by those on NE-DOX and on Free DOX (Figure 6C). Similarly, the level of IgG1 isotype was also decreased in these groups. In contrast, the level of IgG2 isotype increased maximally in the SA-NCs-DOX-treated group followed by the NE-DOX ($P < 0.001$) and Free DOX groups, compared with the infected controls.

NE-DOX and SA-NCs-DOX treatment generates a Th1-type cytokine profile, as determined by qRT-PCR

Expression of Th1 and Th2 cytokines was evaluated by qRT-PCR on day 30 of treatment. The iNOS transcript was up-regulated in the NE-DOX ($P < 0.05$) and SA-NCs-DOX groups (Figure 7). The expression of TNF- α , IFN- λ and IL-12 were elevated in all treated groups, compared that in the *L. donovani*-infected and untreated group. In contrast, the expression of TGF- β was down-regulated in the hamsters treated with NE-DOX and SA-NCs-DOX. IL-4 and IL-10, which are associated with progressive VL, were down-regulated in infected hamsters treated with SA-NCs-DOX while, after NE-DOX treatment, their expression was equivalent to that in infected control.

On the other hand, control NE and control SA-NCs groups exhibited a cytokine response similar to that of infected untreated animals. Free DOX treatment-induced TNF- α , IFN- γ ($P < 0.05$) and IL-12 and inhibited TGF- β , although the level of IL-4 and IL-10 was found to be elevated and comparable to that in the infected group.

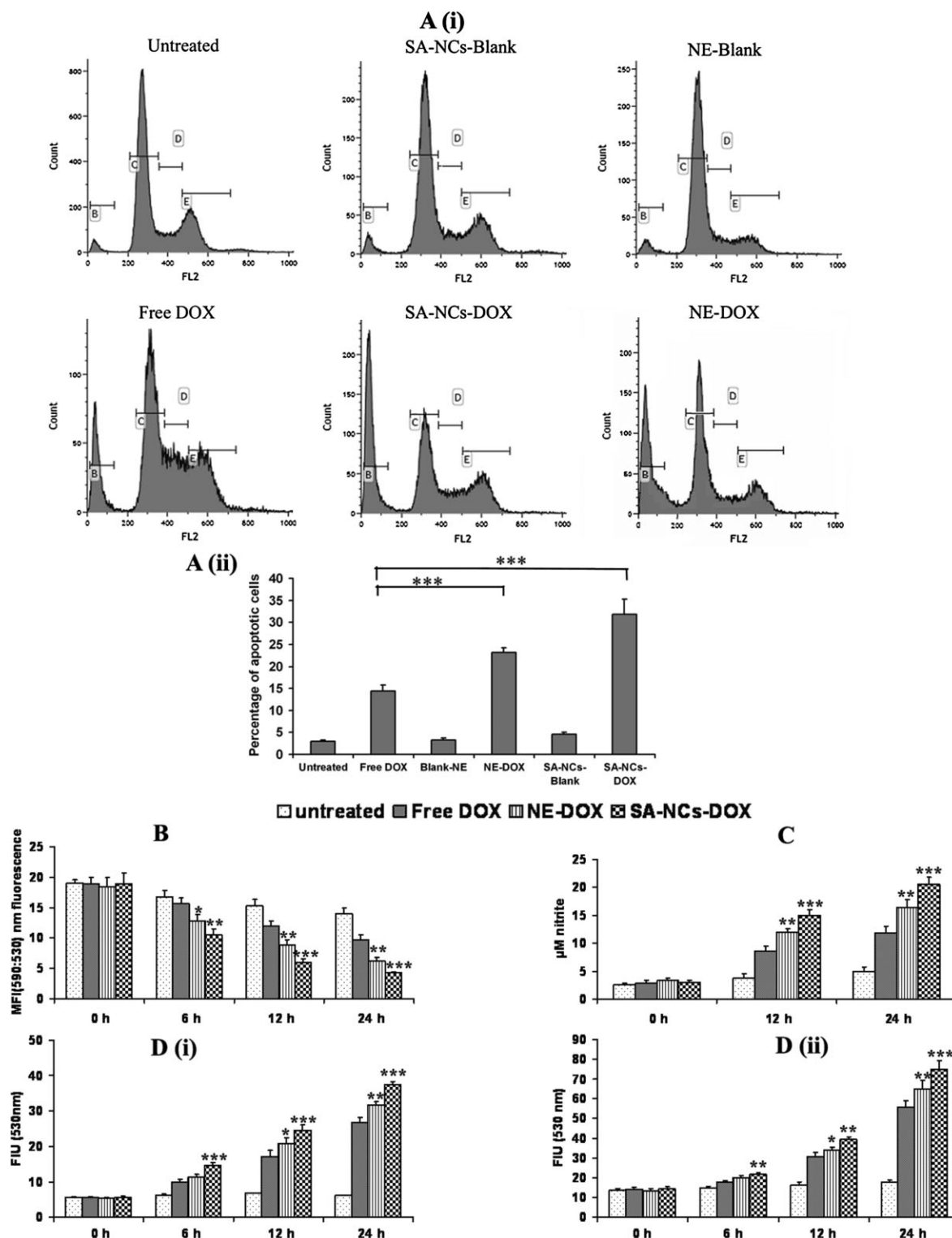


Figure 4

(Ai and ii) Measurement of apoptosis induced by DOX formulations. 10^6 promastigotes were treated with $0.5 \mu\text{g}\cdot\text{mL}^{-1}$ of each of the free drug, NE-DOX and SA-NCs-DOX for 24 h, stained with PI and cell cycle analysis was done by flow cytometer. B, C, D and E gates represent cells in sub G1, G0/G1, S and G2/M phase respectively. Bar graph represents the percentage of cells in sub G1 region undergoing apoptosis after treatment with different formulations. (B) Decrease in $\Delta\psi\text{m}$ in promastigotes following treatment with SA-NCs-DOX, NE-DOX and free DOX for the indicated times and staining with the potentiometric probe JC-1 (10 mM). $\Delta\psi\text{m}$ values are expressed as the ratio of 590:530 nm fluorescence. Assessment of the generation of NO in infected macrophages (C) and ROS generation in promastigotes (Di) and infected macrophages (Dii) at different times after treatment. * $P < 0.05$; ** $P < 0.01$; *** $P < 0.001$, significantly different from Free DOX and from NE-DOX-treated cells.

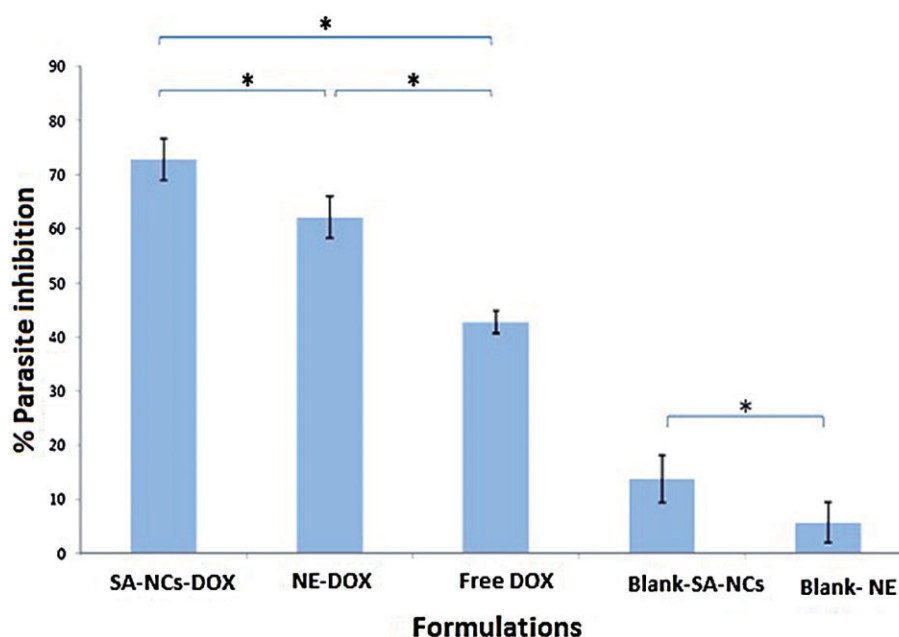


Figure 5

Anti-leishmanial activity of DOX formulations against established infection of *L. donovani* in hamsters. Drug formulations (equivalent to 250 $\mu\text{g}\cdot\text{kg}^{-1}\cdot\text{per day}$ for 4 consecutive days) and formulations without drug (Blank) were injected i.p. into each hamster on day 31 post infection. Parasite burden was estimated by splenic biopsy on day 30 post-treatment and percentage of parasite inhibition was calculated in comparison with the parasite burden of untreated animals. Data shown are means \pm SD ($n = 3$). * $P < 0.05$, significantly different as indicated).

Discussion and conclusion

This study demonstrates that surface coating of DOX-loaded NCs with alginate significantly enhanced the immunological responses through a Th1 pathway, and provided a better management of VL. Recently, formulations of LBL self-assembled polyelectrolyte shells have gained significant attention as a new class of particulate drug delivery system, capable of carrying high payloads of drug to the target site (Shukla *et al.*, 2010). Particle surface chemistry has an important role in Sukhorukov cell particle interactions. The self-assembly provides a convenient method to control the surface composition of the polyelectrolyte shells. In the present study, we developed LBL shells with a variety of surface compositions, providing a wide spectrum of charge properties. The low-energy emulsification method (Liu *et al.*, 2006) was used to prepare the NE core followed by deposition of oppositely charged polyelectrolytes to form the NCs.

The *Leishmania* parasite resides in the host macrophages, where it grows and multiplies as it is protected from the hostile environment of the host defence system. This proliferation inhibits macrophage activation and thereby reducing the release of a range of cytotoxic cytokines. It is known that the macrophage can kill the parasite by releasing cytokines such as TNF- α , IFN- γ , IL-12, and NO, while decreasing the release of IL-10, through the innate immune response (Murray *et al.*, 2003b; Sundar *et al.*, 2004). Treatment strategies that are based on modulation of the immune response, in addition to chemotherapy, result in improved efficacy during infection. In general, the combination of anti-leishmanial drugs with drug carriers has increased their effi-

cacy and this fact has been mainly attributed to an increase in its direct anti-leishmanial action allowing higher drug levels to be attained in the infected macrophages. However, the activation of macrophages by formulation excipients such as the alginates, as we have used in the present study along with chemotherapy is likely to improve the anti-leishmanial activity of macrophages *in vitro* and *in vivo*.

A variety of biopolymers such as alginate or chitosan, are known to show predictable activation of macrophages. Thus alginate exhibited macrophage-activating properties when injected i.p. and high levels of NO and TNF- α release were found in macrophages after exposure to high MW chitosan and oligochitosan. There is significantly increase in cell Numbers of macrophages, lymphocytes and TNF- α secretion were all increased when alginate poly-L-lysine microcapsules were implanted in the peritoneal cavity (Son *et al.*, 2001; Yu *et al.*, 2004; Yang and Jones, 2009). Iwamoto *et al.* (2005) have shown that unsaturated alginate oligomers stimulated RAW 264.7 cells to secrete elevated amounts of IL-1 α , IL-1 β , IL-6 and TNF- α (Iwamoto *et al.*, 2005).

Following the suggestion that immunostimulation could be coupled with chemotherapy to produce an improved effect on visceral infection, we proposed that SA-NCs-DOX would stimulate the innate immune system by activating macrophages. Our results confirmed and extended previous studies confirming that alginate stimulates secretion of inflammatory cytokines. In the present investigation, the pre-formed NE core serves as template for successive deposition of PRM-SA layers, which ultimately leads to the formation of NCs in a LBL fashion with SA as outer covering. The method of complex conservation was used to form a capsule shell

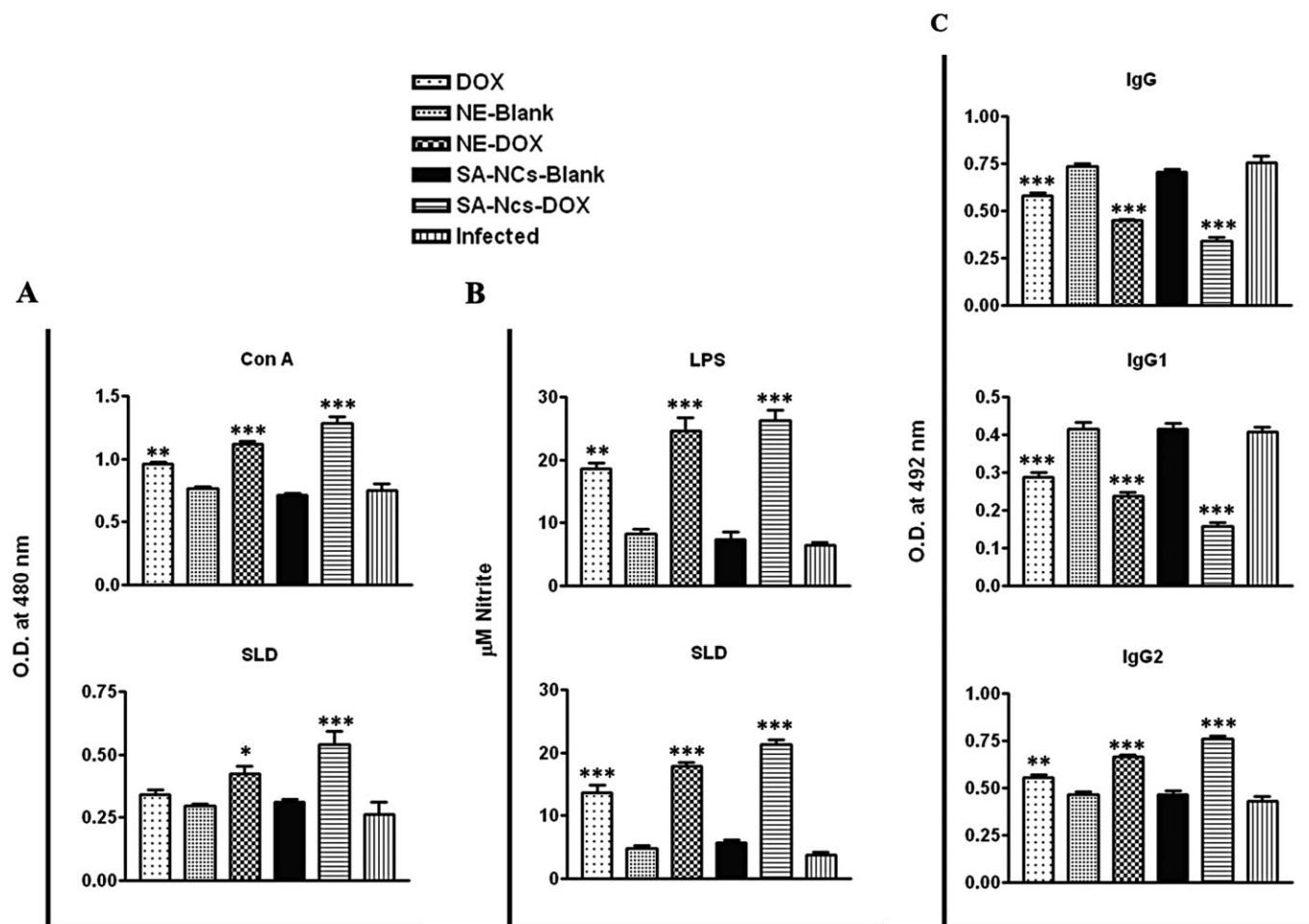


Figure 6

(A) LTT of mononuclear cells (lymph nodes) of *L. donovani*-infected and -treated hamsters, in response to ConA and SLD at 10 mg·mL⁻¹. Proliferation is represented as mean OD of stimulated culture-mean OD of unstimulated control. Each bar represents pooled data (mean + SD) of five hamsters and the data represent the means of triplicate wells + SD. (B) Nitrite production (mM) on day 30 by peritoneal macrophages of hamsters primed with supernatants of lymphocytes of infected and differently treated groups in response to LPS and SLD at 10 mg·mL⁻¹ after 24 h stimulation. The absorbance of the reaction product was measured at 540 nm using Griess reagent; (C) Leishmania-specific IgG and its isotype response on day 30 of treatment. Each bar represents pooled data (mean + SD value) of three replicates. **P* < 0.05; ***P* < 0.01; ****P* < 0.001, significant effects of treatment.

consisting of PRM-SA layers interlinked as a polyelectrolyte complex. The alternating coating of PRM and SA over the NE core was confirmed by reversal of ζ potential at each layering, which resulted in formation of alginate coated NCs (SA-NCs).

To evaluate the effect of SA-NCs-DOX, comparative uptake studies on macrophage cell lines were performed. Figure 3 shows comparative uptake of SA-NCs-DOX and NE-DOX formulations by flow cytometry. This figure indicates almost 1.5-fold greater uptake of SA-NCs-DOX in cell lines compared with NE-DOX. This finding suggests that SA-NCs-DOX undergo electrostatic interactions with relatively negative charged cell membrane. Several researchers have reported that cationic microparticles increase the phagocytosis by dendritic cells and macrophages, in comparison with other charged surfaces (Thiele *et al.*, 2001; Wischke *et al.*, 2006). The mechanism involved for enhanced uptake of positively charged microparticles is the electrostatic attrac-

tion between this cationic substrate and the negatively charged cell surface leading to binding and subsequent internalization. Free DOX, NE-DOX and SA-NCs-DOX were tested for anti-leishmanial activity *in vitro* by determining the percentage killing against intramacrophagic amastigotes. Both the formulations, NE-DOX and SA-NCs-DOX showed significant improvement in efficacy, compared with the effects of Free DOX. Similarly SA-NCs-DOX showed significantly better efficacy compared with NE-DOX (Figure 2), which explains the greater action of SA-NCs-DOX against parasites.

DOX causes apoptosis in *Leishmania* parasites (Debrabant *et al.*, 2003) and the present study showed that the entrapment of DOX in SA-coated NCs markedly increased the apoptotic efficiency of this drug *in vitro*. This might be attributed to the higher production of ROS and NO by the SA coating, as ROS generation in the cells following drug treatment is

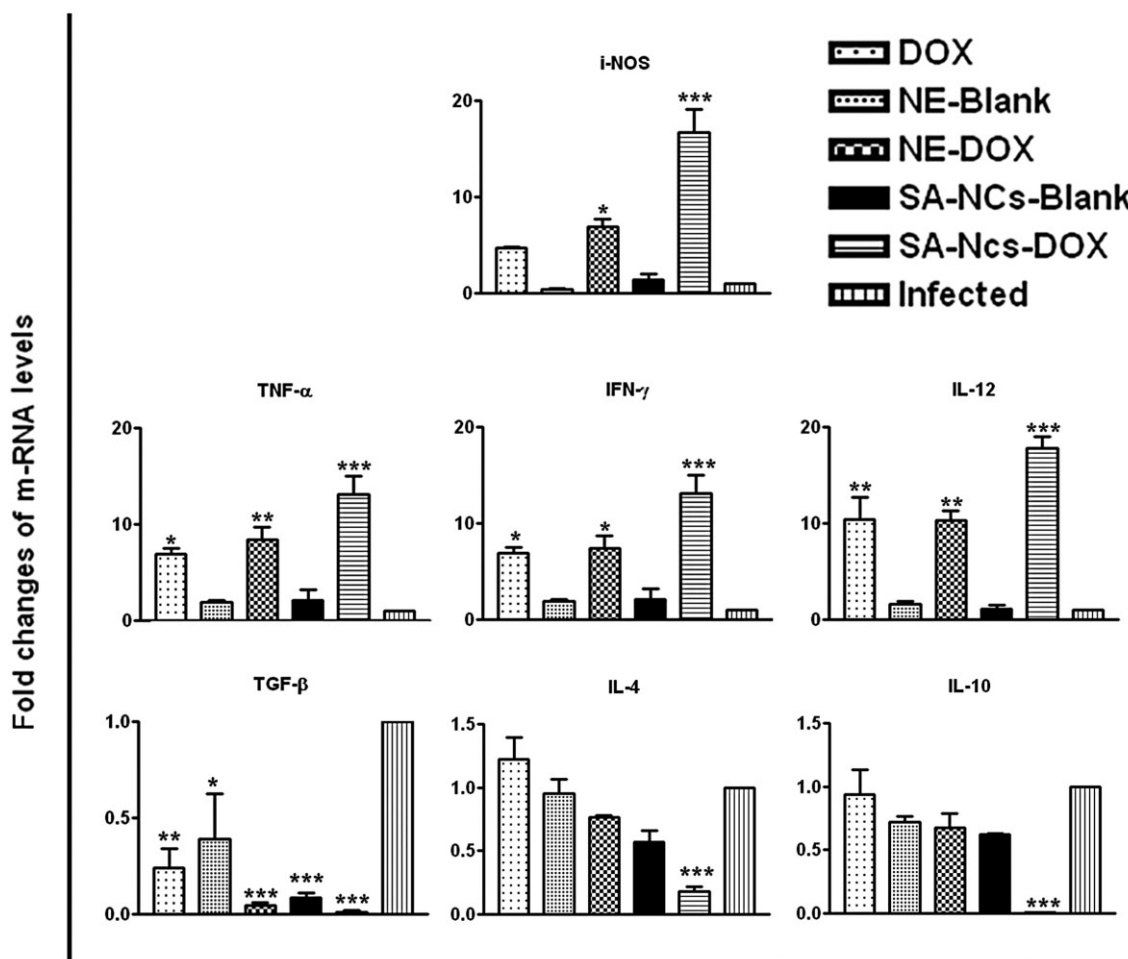


Figure 7

Splenic iNOS and cytokine mRNA expression profile analysis of treated infected hamsters with drug formulations (equivalent to 250 $\mu\text{g}\cdot\text{kg}^{-1}$ per day for 4 consecutive days) and formulations without drug on day 30 of treatment by quantitative real-time RT-PCR. * $P < 0.05$; ** $P < 0.01$; *** $P < 0.001$, significant effects of treatment.

known to direct the cells towards apoptosis (Chipuk and Green, 2005).

In parallel to this, we have also carried out *in vivo* studies in hamsters and observed that SA-NCs-DOX, coated with immunomodulatory polymers, have better efficacy than NE-DOX or the Free DOX. As SA attached to the formulation is immunomodulatory, the effect of formulation on immune parameters of hamsters was further assessed. *Leishmania*-specific lymphoproliferative assay (LTT) and NO production are measures of cell-mediated immunity (CMI), which almost always accompanies the control of parasite growth and healing. Nevertheless, it is not LTT itself that is the primary effector mechanism of immunity, but rather the stimulation of *Leishmania*-specific T-cells to develop macrophage-activating factors, which in turn activate macrophages for the destruction of the intracellular parasites. This is consistent with the critical role of NO-mediated macrophage effector mechanism, which is known to control parasite replication in this animal model (Garg *et al.*, 2006).

Apart from weakened cellular responses; VL is linked with the production of a high level of antibody, which is observed

prior to the detection of a parasite-specific T-cell response. It is well established that titres of IgG and IgG1 antibodies increase with *L. donovani* load. The lowest level of these antibodies is therefore consistent with the decreased parasite loads noticed in the SA-NCs-DOX-treated group and the better protective response, compared with the other treated groups. The substantial increase in IgG2 levels in SA-NCs-DOX-treated animals is also indicative of enhanced CMI (Samant *et al.*, 2009).

To test whether the enhanced efficacy of DOX against VL *in vivo* was coupled with immuno-stimulation following attachment of SA-NCs, the cytokine profile (TNF- α , IL-12 and IFN- γ) along with iNOS level was determined by real-time PCR and compared with that in NE-DOX-treated animals. The Th1-type of cell-mediated immunological response is responsible for protection against VL, while a Th2 type of response exacerbates the disease. The transcript of IFN- γ , a cytokine characteristic of the Th1-type response that has a dominant effect on macrophage microbicidal responses and other effector killing mechanisms, along with TNF- α , often reported to act in concert to activate iNOS for the production

of NO (Liew *et al.*, 1990) were down-regulated in infected hamsters, whereas their expression was increased many-fold in the infected hamsters treated with NE-DOX and SA-NCs-DOX. The key macrophage-deactivating, Th1-suppressive, cytokines, IL-10 and IL-4, are reported to have a definite association with an acute phase of VL during which a progressive increase of IL-10 and IL-4 transcripts in tissues were generated, but were not detectable after a successful cure (Ghalib *et al.*, 1993; Melby *et al.*, 1998). Compatible with these results, IL-10 and IL-4 mRNA levels were markedly down-regulated in hamsters treated with SA-NCs-DOX, compared with those in infected but untreated hamsters, (Noben-Trauth *et al.*, 2003), but on the contrary both cytokines were expressed at high level in NE-DOX and Free DOX groups.

It has been reported that IL-10-deficient mice require IFN- γ , that is largely induced by IL-12, in order to generate primary Th1 cell-mediated anti-leishmanial activity (Murray *et al.*, 2000; Basu *et al.*, 2005). In the present study, IL-12 was completely down-regulated in infected hamsters; whereas high levels of IL-12 mRNA was observed in transcripts found in Free DOX, NE-DOX and SA-NCs-DOX groups. TGF- β is a pleiotropic cytokine involved in many functions of resident tissue cells, but for the most part, inhibiting some activity of immune cells. TGF- β can mediate immunosuppression by inhibiting IL-2-dependent T- and B-cell proliferation and IL-2-dependent antibody production by B-cells (Kehrl *et al.*, 1986). Studies have suggested the role of this cytokine is to maintain or to exacerbate the characteristic immunosuppression observed in this disease (Rodrigues *et al.*, 1998). In our experiments, TGF- β was strongly inhibited in all drug-treated groups, in comparison to infected controls.

In summary, this study has shown the SA-NCs-DOX to elicit strong Th1 responses with up-regulation of iNOS, TNF- α and IFN- γ and down-regulation of TGF- β , IL-4 and IL-10, while NE-DOX and Free DOX-induced mixed Th1/Th2 types of response. These results correlate with the data of parasite load measured in these groups in which the highest inhibition was observed in the SA-NCs-DOX group followed by the NE-DOX and the Free DOX groups.

As strong immunosuppression accompanies *L. donovani* infection, a better and more effective strategy for the optimum efficacy of anti-leishmanial drugs should incorporate both the direct killing of parasites by the drug along with concurrent generation of immunity against the disease. The SA-NCs-DOX-induced safe parasite killing through more efficient apoptosis and also effectively switched on immune responses in the host, specific to the parasite. Thus, this formulation may serve as a promising and low-cost alternative to expensive lipid-based formulations for treatment of VL.

Acknowledgement

P. R. M. is grateful to the Council for Scientific and Industrial Research New Delhi, India for providing financial support under the Network Project (BIOCERAM ESC-0103 and NanoSHE BSC 0112). S. K. and R. T. are grateful to the Indian Council of Medical Research, New Delhi, India and CSIR, New Delhi, India for providing SRF fellowships. The authors

are particularly grateful to Mr. Vishwakarma, SAIF, CDRI, Lucknow for providing Flow Cytometry study and Dr. Ambak Kumar Rai for his critical suggestions during execution of experiments. This is CDRI Communication number 8669.

Author contributions

P. R. M. and A. D. conceived and designed and facilitated the study, ethical approval, and S. K., A. V. and R. V. conducted formulation and characterization of NCs; R. T., P. M. and A. K. C. managed the *in vivo* and *in vitro* studies involving *L. donovani*; P. R. M., A. D., P. R. P. V. and S. K. analysed the data and prepared the first draft of the paper; P. R. M., A. D., A. V., R. V. and S. K. all reviewed and critically appraised the paper; P. R. M. had primary responsibility for the final content of the paper; and all authors agreed on the final version.

Conflict of interest

The authors declare that they have not any conflict of interest.

References

- Albright CF, Graciani N, Han W, Yue E, Stein R, Lai Z *et al.* (2005). Matrix metalloproteinase-activated doxorubicin prodrugs inhibit HT1080 xenograft growth better than doxorubicin with less toxicity. *Mol Cancer Ther* 4: 751–760.
- Basu R, Bhaumik S, Basu JM, Naskar K, De T, Roy S (2005). Kinoplastid membrane protein-11 DNA vaccination induces complete protection against both pentavalent antimonial-sensitive and -resistant strains of *Leishmania donovani* that correlates with inducible nitric oxide synthase activity and IL-4 generation: evidence for mixed Th1- and Th2-like responses in visceral leishmaniasis. *J Immunol* 174: 7160–7171.
- Chipuk JE, Green DR (2005). Do inducers of apoptosis trigger caspase-independent cell death? *Nat Rev Mol Cell Biol* 6: 268–275.
- Debrabant A, Lee N, Bertholet S, Duncan R, Nakhasi HL (2003). Programmed cell death in trypanosomatids and other unicellular organisms. *Int J Parasitol* 33: 257–267.
- Dey R, Moraes CT (2000). Lack of oxidative phosphorylation and low mitochondrial membrane potential decrease susceptibility to apoptosis and do not modulate the protective effect of Bcl-x(L) in osteosarcoma cells. *J Biol Chem* 275: 7087–7094.
- Duranteau J, Chandel NS, Kulisz A, Shao Z, Schumacker PT (1998). Intracellular signaling by reactive oxygen species during hypoxia in cardiomyocytes. *J Biol Chem* 273: 11619–11624.
- Duverger A, Jackson RJ, van Ginkel FW, Fischer R, Tafaro A, Leppla SH *et al.* (2006). *Bacillus anthracis* edema toxin acts as an adjuvant for mucosal immune responses to nasally administered vaccine antigens. *J Immunol* 176: 1776–1783.
- Garg R, Gupta SK, Tripathi P, Hajela K, Sundar S, Naik S *et al.* (2006). *Leishmania donovani*: identification of stimulatory soluble

antigenic proteins using cured human and hamster lymphocytes for their prophylactic potential against visceral leishmaniasis. *Vaccine* 24: 2900–2909.

Ghalib HW, Piuvezam MR, Skeiky YA, Siddig M, Hashim FA, el Hassan AM *et al.* (1993). Interleukin 10 production correlates with pathology in human *Leishmania donovani* infections. *J Clin Invest* 92: 324–329.

Ghosh S, Debnath S, Hazra S, Hartung A, Thomale K, Schultheis M *et al.* (2011). *Valeriana wallichii* root extracts and fractions with activity against *Leishmania* spp. *Parasitol Res* 108: 861–871.

Gupta GK, Kansal S, Misra P, Dube A, Mishra PR (2009). Uptake of biodegradable gel-assisted LBL nanomatrix by *Leishmania donovani*-infected macrophages. *AAPS PharmSciTech* 10: 1343–1347.

Gupta R, Kushawaha PK, Samant M, Jaiswal AK, Baharia RK, Dube A (2011). Treatment of *Leishmania donovani*-infected hamsters with miltefosine: analysis of cytokine mRNA expression by real-time PCR, lymphoproliferation, nitrite production and antibody responses. *J Antimicrob Chemother* 67: 440–443.

Guru PY, Agrawal AK, Singha UK, Singhal A, Gupta CM (1989). Drug targeting in *Leishmania donovani* infections using tuftsin-bearing liposomes as drug vehicles. *FEBS Lett* 245: 204–208.

Haldar AK, Sen P, Roy S (2011). Use of antimony in the treatment of leishmaniasis: current status and future directions. *Mol Biol Int* 2011: S71242.

Hartmann G, Vassileva V, Piquette-Miller M (2005). Impact of endotoxin-induced changes in P-glycoprotein expression on disposition of doxorubicin in mice. *Drug Metab Dispos* 33: 820–828.

Higuchi M, Higashi N, Taki H, Osawa T (1990). Cytolytic mechanisms of activated macrophages. Tumor necrosis factor and L-arginine-dependent mechanisms act synergistically as the major cytolytic mechanisms of activated macrophages. *J Immunol* 144: 1425–1431.

Hussner J, Ameling S, Hammer E, Herzog S, Steil L, Schwebe M *et al.* (2012). Regulation of interferon-inducible proteins by doxorubicin via interferon gamma-Janus tyrosine kinase-signal transducer and activator of transcription signaling in tumor cells. *Mol Pharmacol* 81: 679–688.

Iwamoto M, Kurachi M, Nakashima T, Kim D, Yamaguchi K, Oda T *et al.* (2005). Structure-activity relationship of alginate oligosaccharides in the induction of cytokine production from RAW264.7 cells. *FEBS Lett* 579: 4423–4429.

Kansal S, Tandon R, Dwivedi P, Misra P, Verma PR, Dube A *et al.* (2012). Development of nanocapsules bearing doxorubicin for macrophage targeting through the phosphatidylserine ligand: a system for intervention in visceral leishmaniasis. *J Antimicrob Chemother* 67: 2650–2660.

Kataoka K, Matsumoto T, Yokoyama M, Okano T, Sakurai Y, Fukushima S *et al.* (2000). Doxorubicin-loaded poly(ethylene glycol)-poly(beta-benzyl-L-aspartate) copolymer micelles: their pharmaceutical characteristics and biological significance. *J Control Release* 64: 143–153.

Kehrl JH, Roberts AB, Wakefield LM, Jakowlew S, Sporn MB, Fauci AS (1986). Transforming growth factor beta is an important immunomodulatory protein for human B lymphocytes. *J Immunol* 137: 3855–3860.

Kilkenny C, Browne W, Cuthill IC, Emerson M, Altman DG (2010). Animal research: reporting *in vivo* experiments: the ARRIVE Guidelines. *Br J Pharmacol* 160: 1577–1579.

Liew FY, Li Y, Millott S (1990). Tumor necrosis factor-alpha synergizes with IFN-gamma in mediating killing of *Leishmania* major through the induction of nitric oxide. *J Immunol* 145: 4306–4310.

Liu W, Sun D, Li C, Liu Q, Xu J (2006). Formation and stability of paraffin oil-in-water nano-emulsions prepared by the emulsion inversion point method. *J Colloid Interface Sci* 303: 557–563.

Luanpitpong S, Chanvorachote P, Nimmannit U, Leonard SS, Stehlik C, Wang L *et al.* (2012). Mitochondrial superoxide mediates doxorubicin-induced keratinocyte apoptosis through oxidative modification of ERK and Bcl-2 ubiquitination. *Biochem Pharmacol* 83: 1643–1654.

McGrath J, Drummond G, McLachlan E, Kilkenny C, Wainwright C (2010). Guidelines for reporting experiments involving animals: the ARRIVE guidelines. *Br J Pharmacol* 160: 1573–1576.

Melby PC, Tryon VV, Chandrasekar B, Freeman GL (1998). Cloning of Syrian hamster (*Mesocricetus auratus*) cytokine cDNAs and analysis of cytokine mRNA expression in experimental visceral leishmaniasis. *Infect Immun* 66: 2135–2142.

Mukherjee S, Das L, Kole L, Karmakar S, Datta N, Das PK (2004). Targeting of parasite-specific immunoliposome-encapsulated doxorubicin in the treatment of experimental visceral leishmaniasis. *J Infect Dis* 189: 1024–1034.

Murray HW, Montelibano C, Peterson R, Sypek JP (2000). Interleukin-12 regulates the response to chemotherapy in experimental visceral *Leishmaniasis*. *J Infect Dis* 182: 1497–1502.

Murray HW, Brooks EB, DeVecchio JL, Heinzel FP (2003a). Immunoenhancement combined with amphotericin B as treatment for experimental visceral leishmaniasis. *Antimicrob Agents Chemother* 47: 2513–2517.

Murray HW, Moreira AL, Lu CM, DeVecchio JL, Matsuhashi M, Ma X *et al.* (2003b). Determinants of response to interleukin-10 receptor blockade immunotherapy in experimental visceral leishmaniasis. *J Infect Dis* 188: 458–464.

Noben-Trauth N, Lira R, Nagase H, Paul WE, Sacks DL (2003). The relative contribution of IL-4 receptor signaling and IL-10 to susceptibility to *Leishmania* major. *J Immunol* 170: 5152–5158.

Oliveira LF, Schubach AO, Martins MM, Passos SL, Oliveira RV, Marzochi MC *et al.* (2011). Systematic review of the adverse effects of cutaneous leishmaniasis treatment in the New World. *Acta Trop* 118: 87–96.

Pal R, Rizvi SY, Kundu B, Mathur KB, Katiyar JC (1991). *Leishmania donovani* in hamsters: stimulation of non-specific resistance by some novel glycopeptides and impact on therapeutic efficacy. *Experientia* 47: 486–490.

Porporatto C, Bianco ID, Riera CM, Correa SG (2003). Chitosan induces different L-arginine metabolic pathways in resting and inflammatory macrophages. *Biochem Biophys Res Commun* 304: 266–272.

Riccardi C, Nicoletti I (2006). Analysis of apoptosis by propidium iodide staining and flow cytometry. *Nat Protoc* 1: 1458–1461.

Rodrigues V Jr, Santana da Silva J, Campos-Neto A (1998). Transforming growth factor beta and immunosuppression in experimental visceral leishmaniasis. *Infect Immun* 66: 1233–1236.

Samant M, Gupta R, Kumari S, Misra P, Khare P, Kushawaha PK *et al.* (2009). Immunization with the DNA-encoding N-terminal domain of proteophosphoglycan of *Leishmania donovani* generates Th1-type immunoprotective response against experimental visceral leishmaniasis. *J Immunol* 183: 470–479.

- Sett R, Basu N, Ghosh AK, Das PK (1992). Potential of doxorubicin as an anti-leishmanial agent. *J Parasitol* 78: 350–354.
- Seymour AA, Sheldon JH, Smith PL, Asaad M, Rogers WL (1994). Potentiation of the renal responses to bradykinin by inhibition of neutral endopeptidase 3.4.24.11 and angiotensin-converting enzyme in anesthetized dogs. *J Pharmacol Exp Ther* 269: 263–270.
- Shukla P, Gupta G, Singodia D, Shukla R, Verma AK, Dwivedi P *et al.* (2010). Emerging trend in nano-engineered polyelectrolyte-based surrogate carriers for delivery of bioactives. *Expert Opin Drug Deliv* 7: 993–1011.
- Singh G, Dey CS (2007). Induction of apoptosis-like cell death by pentamidine and doxorubicin through differential inhibition of topoisomerase II in arsenite-resistant *L. donovani*. *Acta Trop* 103: 172–185.
- Singodia D, Khare P, Dube A, Talegaonkar S, Khar RK, Mishra PR (2011). Development and performance evaluation of alginate-capped amphotericin B lipid nanoconstructs against visceral leishmaniasis. *J Biomed Nanotechnol* 7: 123–124.
- Son EH, Moon EY, Rhee DK, Pyo S (2001). Stimulation of various functions in murine peritoneal macrophages by high mannuronic acid-containing alginate (HMA) exposure *in vivo*. *Int Immunopharmacol* 1: 147–154.
- Soto M, Iborra S, Quijada L, Folgueira C, Alonso C, Requena JM (2004). Cell-cycle-dependent translation of histone mRNAs is the key control point for regulation of histone biosynthesis in *Leishmania infantum*. *Biochem J* 379 (Pt 3): 617–625.
- Sudhandiran G, Shaha C (2003). Antimonial-induced increase in intracellular Ca^{2+} through non-selective cation channels in the host and the parasite is responsible for apoptosis of intracellular *Leishmania donovani* amastigotes. *J Biol Chem* 278: 25120–25132.
- Sundar S, Rai M (2002). Advances in the treatment of leishmaniasis. *Curr Opin Infect Dis* 15: 593–598.
- Sundar S, Mehta H, Suresh AV, Singh SP, Rai M, Murray HW (2004). Amphotericin B treatment for Indian visceral leishmaniasis: conventional versus lipid formulations. *Clin Infect Dis* 38: 377–383.
- Tandon R, Misra P, Soni VK, Bano N, Misra-Bhattacharya S, Dube A (2012). Unresponsiveness of *Mycobacterium w* vaccine in managing acute and chronic *Leishmania donovani* infections in mouse and hamster. *Parasitology* 140: 435–444.
- Thiele L, Rothen-Rutishauser B, Jilek S, Wunderli-Allenspach H, Merkle HP, Walter E (2001). Evaluation of particle uptake in human blood monocyte-derived cells *in vitro*. Does phagocytosis activity of dendritic cells measure up with macrophages? *J Control Release* 76: 59–71.
- Tiuman TS, Santos AO, Ueda-Nakamura T, Filho BP, Nakamura CV (2011). Recent advances in leishmaniasis treatment. *Int J Infect Dis* 15: e525–e532.
- Wischke C, Borchert HH, Zimmermann J, Siebenbrodt I, Lorenzen DR (2006). Stable cationic microparticles for enhanced model antigen delivery to dendritic cells. *J Control Release* 114: 359–368.
- Yang D, Jones KS (2009). Effect of alginate on innate immune activation of macrophages. *J Biomed Mater Res A* 90: 411–418.
- Yu Z, Zhao L, Ke H (2004). Potential role of nuclear factor-kappaB in the induction of nitric oxide and tumor necrosis factor-alpha by oligochitosan in macrophages. *Int Immunopharmacol* 4: 193–200.